

Remote Monitoring of Vegetation using a Fluorescence Lidar System in Spectrally Resolving and Multi-Spectral Imaging Modes

H. Edner, J. Johansson, P. Ragnarson, S. Svanberg and E. Wallinder

Department of Physics, Lund Institute of Technology
P.O. Box 118, S-221 00 Lund, Sweden
(tel. 46-46-2227650, fax 46-46-2224250)

ABSTRACT

Remote measurements with a fluorescence lidar system on spruce and maize during a LASFLEUR field campaign at DLR, Oberpfaffenhofen, are reported. The system could be used in a spectrally resolving mode yielding the full fluorescence spectrum in a selected point or in an imaging mode, where spatially resolved data could be captured simultaneously in four selected spectral bands. As a transmitter a Nd:YAG laser system operating at 20 Hz was used, utilizing either the frequency tripled output at 355 nm or, preferentially, a Raman shifted output at 397 nm. A 0.40 m diameter telescope was used for collecting fluorescence photons, that were analysed either in an optical multichannel analyser system or in a four-colour imaging system, both equipped with intensified CCD detectors. Detailed laboratory studies of the excitation response of spruce and maize were performed initially, using both shorter and longer excitation wavelengths in addition to the ones given above. 397 nm was found to be the optimal eyesafe wavelength. The daily cycle of spruce and maize was studied remotely for samples under parallel plant physiological scrutiny. Maize grown under different conditions with regard to nutrition and water supply was investigated.

Fluorescence imaging was performed with a maximum distance of 110 m. Detailed studies were made on maize plants at a distance of 30 m. Fluorescence images recorded at selected wavelengths, including the two chlorophyll fluorescence peaks, were recorded for each plant. The simultaneous recording of fluorescence images makes the system less vulnerable to wind movements of the vegetation. Sequential single-colour fluorescence imaging, yielding sharper individual images was also evaluated. The usefulness of spectrally resolving and imaging fluorosensors for remote vegetation status assessment is discussed.

INTRODUCTION

In recent years the effect of environmental pollution on

vegetation has become more obvious. With the increasing awareness of this problem a need for methods of remote detection of early damages on forests has appeared. Satellite multi-spectral reflectance data have shown to be very valuable for land cover assessment and differentiation between plant species [1]. However, for recognition of early stress to vegetation the success has been limited and more accurate techniques are needed. A method which may contribute with additional information is remote laser-induced fluorescence [2]. The first application of this method was the monitoring of marine constituents [3]. The fluorescence from algae, tryptophan and the less well-defined "Gelbstoff" was monitored together with the Raman scattering signal from the OH stretch vibration of water. For these early measurements photomultipliers equipped with interference filters were used as detectors. The same equipment was also briefly tested for terrestrial measurements and showed some promising results [4,5].

Recently there has been a substantial increase in the interest in this field with a variety of different approaches as a result. Optical multi-channel (OMA) detection systems have been used to record full fluorescence spectra in the visible region [6-8], also including the broad-band blue fluorescence from vegetation [6,8]. The ratio of the two chlorophyll fluorescence peaks at 685 and 735 nm, respectively, has since long been known to be higher in stressed plants [9]. Due to a preferential fluorescence reabsorption of the 685 nm peak, this ratio changes with chlorophyll concentration in the leaves. By including the blue and green fluorescence, additional information about the condition of plants may be achieved. The origin of the blue fluorescence is still quite unclear, since most biomolecules exhibit some fluorescence in the blue spectral region. Among several fluorophores, carotenoids [10], riboflavin [10], cinnamic acids [11], coumarin [11] and NADPH [12,13] have been mentioned. Another approach is to measure the time-resolved chlorophyll fluorescence from the plants [13,14]. The fluorescence lifetime is longer for stressed plants, probably due to a partially blocked electron transport of the photosynthesis.

This technique requires the simultaneous recording of the scattered laser light from the object to be able to correct for the different arrival times of the fluorescence photons from different leaves within an object. These new techniques have become possible because of the rapid advances in detector systems for fluorescence spectroscopy. CCD cameras with single-photon counting capability are available for spectral as well as imaging measurements. These have, besides a high quantum yield, a binning capability, which allows the operator to freely make a trade off between resolution and signal intensity. Furthermore, advances in laser technology will allow measurement at a longer range than what has been possible before. An operating range of 300 m with single-shot readout seems very realistic today.

In this paper the results from a joint LASFLEUR field campaign in Oberpfaffenhofen, Germany, during July 1992, will be presented. Detailed laboratory studies of the excitation response of spruce and maize were performed initially, using excitation wavelengths ranging from 320 nm up to 450 nm. 397 nm was found to be the optimal eyesafe wavelength. The daily cycle of spruce and maize was studied remotely for samples under parallel plant physiological scrutiny. Furthermore, maize grown under different conditions with regard to nutrition and water supply was investigated. The fluorescence data were found to correlate well with chlorophyll content of the plants. The measurements

were performed using either a spectrally resolving OMA system or a multi-colour imaging system with simultaneous image recording at four selected wavelengths. Switching between the two measurement modes could be done rapidly facilitating measurements on the same target in both modes. A system description has appeared in Ref. 15.

MATERIAL AND METHODS

The laser transmitter of the lidar system is a Nd:YAG laser with frequency doubling/tripling. The mobile lidar system originally uses a dye laser, pumped by the Nd:YAG laser. The outgoing beam is directed coaxially with a vertically mounted 0.40 m diameter telescope and transmitted towards the target via a large flat mirror in a retractable transmitting/receiving dome on the roof. Computer controlled stepper motors are used to turn the dome and to tilt the mirror. A video camera is used to provide an image of the target area. When used in the field, the system is supplied with electric power from a 20 kW Diesel motor generator, which is housed in a trailer towed by the truck. A photograph of the lidar van at the experiment site is shown in Fig. 1.

In order to induce chlorophyll fluorescence efficiently while still staying eyesafe, the output from the frequency-tripled Nd:YAG laser (355 nm, 200 mJ pulse energy) was Raman-

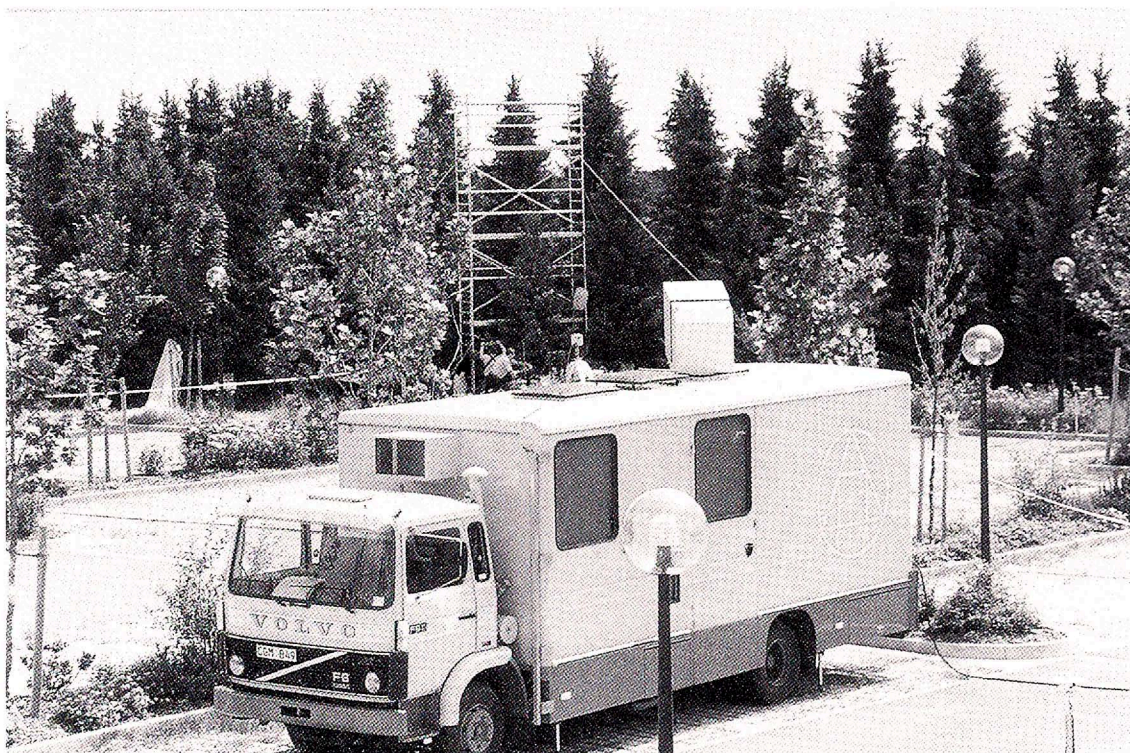


Fig. 1 - Photograph of the lidar van at the measurement site in Oberpfaffenhofen, Germany.

shifted in a high-pressure deuterium cell to generate radiation at 397 nm. An output pulse energy of 30 mJ was achieved at 20 Hz. The radiation was transmitted in a divergent beam towards the target area. The fluorescence light was collected by the lidar telescope and directed into a second, Cassegrainian telescope as shown in Fig. 2. The image plane of the lidar telescope coincided with the object plane of the Cassegrainian telescope. In the image plane of the Cassegrainian telescope an image intensified CCD camera (Spectroscopy Instruments model ICCD-576) was placed. The gate width of the image intensifier was set at 20 ns to efficiently suppress influence of the daylight illumination of the object. The Cassegrainian telescope has its first mirror cut into four segments that can be individually adjusted. By tilting the mirror segments, each segment produces an image at the image intensifier; in total four identical images arranged as four quadrants on the detector. Furthermore, different interference filters or Schott coloured-glass filters were placed before each mirror segment matching specific features of the fluorescence spectra. Such features may include the broad-band fluorescence structures at 450 nm and 520 nm and the chlorophyll fluorescence peaks at 685 nm and 740 nm. The fluorescence images are read out to a PC 486 computer and stored with 14 bit dynamic range.

Computer processing makes it possible to generate a new image, pixel by pixel, from the four sub-images using a suitably designed spectral contrast function, which enhances features of interest. One example of such a spectral contrast function is the ratio $I(685\text{nm})/I(740\text{nm})$, which displays the chlorophyll concentration of the target. The resulting image is shown on the screen in false colour.

Alternatively, fluorescence could be collected pointwise and dispersed in an optical multichannel analyser (OMA). In this mode of operation, a flip-in mirror is used in the optical pathway guiding the fluorescence light into a 600 μm optical quartz fibre. The tip of the fibre was pierced through a white screen in the image plane of the lidar telescope in order to more easily select a small, well defined measurement area within the image. The fluorescence light was guided through the optical fibre and lens coupled to an $f=270$ mm Jarrel Ash spectrometer. The detector was an image intensified 1024 channel diode array from PARC (Model 1421). In this way remote fluorescence spectra were integrated over 500 laser pulses and displayed on the screen of the OMA mainframe (Model 1460). The gating pulse width was about 300 ns during the measurements.

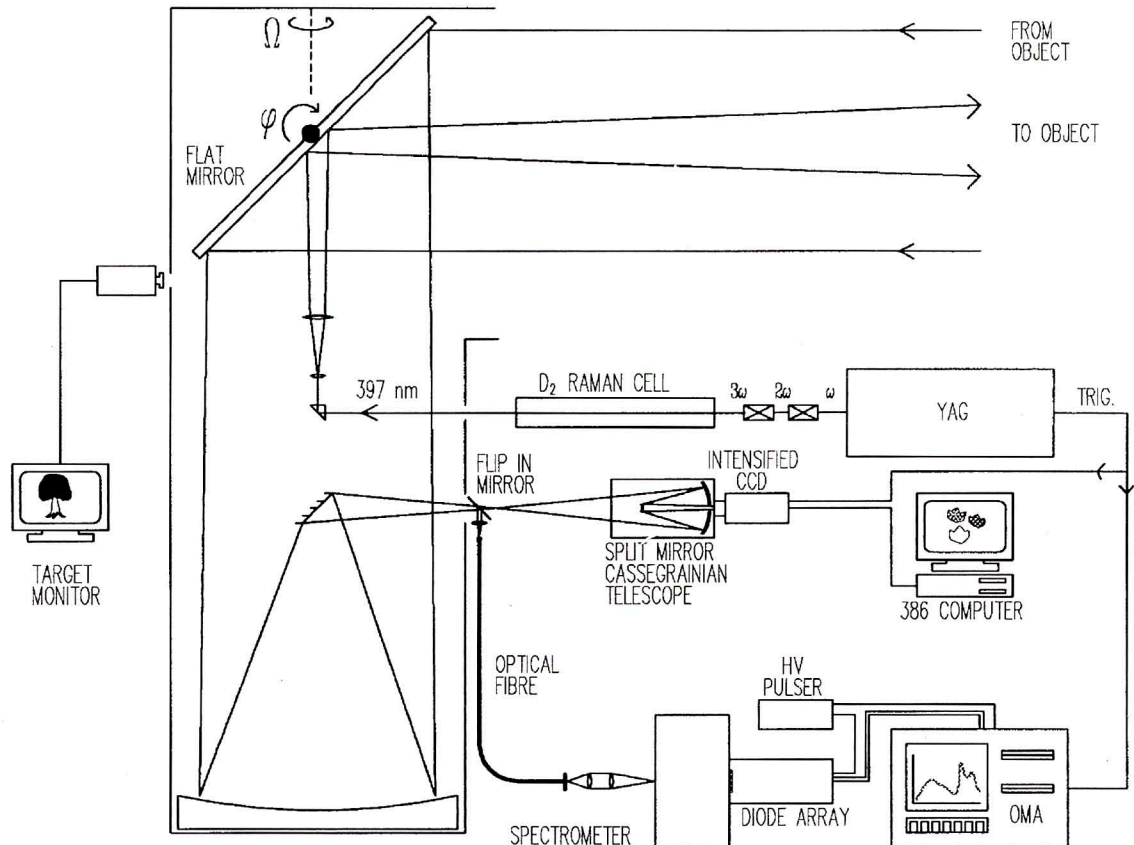


Fig. 2 - Set-up for remote recordings of fluorescence spectra and multi-colour fluorescence images of vegetation. As an excitation source a Raman cell pumped by a frequency tripled YAG laser, was used. The output pulse energy was about 30 mJ/pulse. By using a flip-in mirror switching between the OMA system and the multi-colour imaging system was possible.

RESULTS AND DISCUSSION

An investigation of the influence of different excitation wavelengths was performed for different plant species. The measurements were carried out inside the mobile laboratory to obtain a better signal-to-noise ratio. Different Raman Stokes and anti-Stokes components were selected and transmitted through an optical fibre to the sample. The result for maize plants is shown in Fig. 3. As can be seen, the chlorophyll fluorescence at 685 and 735 nm is efficiently excited for excitation wavelengths in the blue region, whereas for UV excitation the chlorophyll fluorescence is very low. For UV excitation a magnification of the intensity scale reveal a faint chlorophyll fluorescence superimposed on the tail of the blue fluorescence. This interference of the tail of the blue fluorescence with the chlorophyll fluorescence is clearly a problem that has to be taken into account for an accurate determination of the “true” chlorophyll fluorescence. One way to deal with this problem is to utilize the 500-650 nm spectral region to fit the tail of the blue fluorescence in the region between 650 nm and 800 nm, and to subtract this blue fluorescence from the chlorophyll fluorescence.

The blue fluorescence, on the other hand, is better excited with UV light, as shown in Fig. 3. Thus, if one wants to utilize both the blue and the red fluorescence in the fluorescence monitoring, the optimal excitation wavelength for maize is probably in the range between 390-400 nm. Furthermore, eye safety regulations does not allow high power optical radiation in the visible region. Another example of the same measurement is shown in Fig. 4 for needles of a spruce tree. Again the chlorophyll fluorescence is best excited for longer excitation wavelengths. For the UV excitation wavelengths a substantial fluorescence peak appears at about 725 nm. This is, however, probably not only fluorescence originating from chlorophyll. More likely, this structure appears partly due to a very strong fluorescence reabsorption peaking at 670 nm from the chlorophyll pigments. Therefore, one has to be extra careful when evaluation such UV-excited fluorescence spectra.

With the above results in mind, 397 nm excitation was selected for the remote fluorescence measurements. Examples of remote fluorescence spectra from spruce, maize and maple are shown in Fig. 5. A comparison with Figs. 3 and 4 shows a stronger blue fluorescence for the

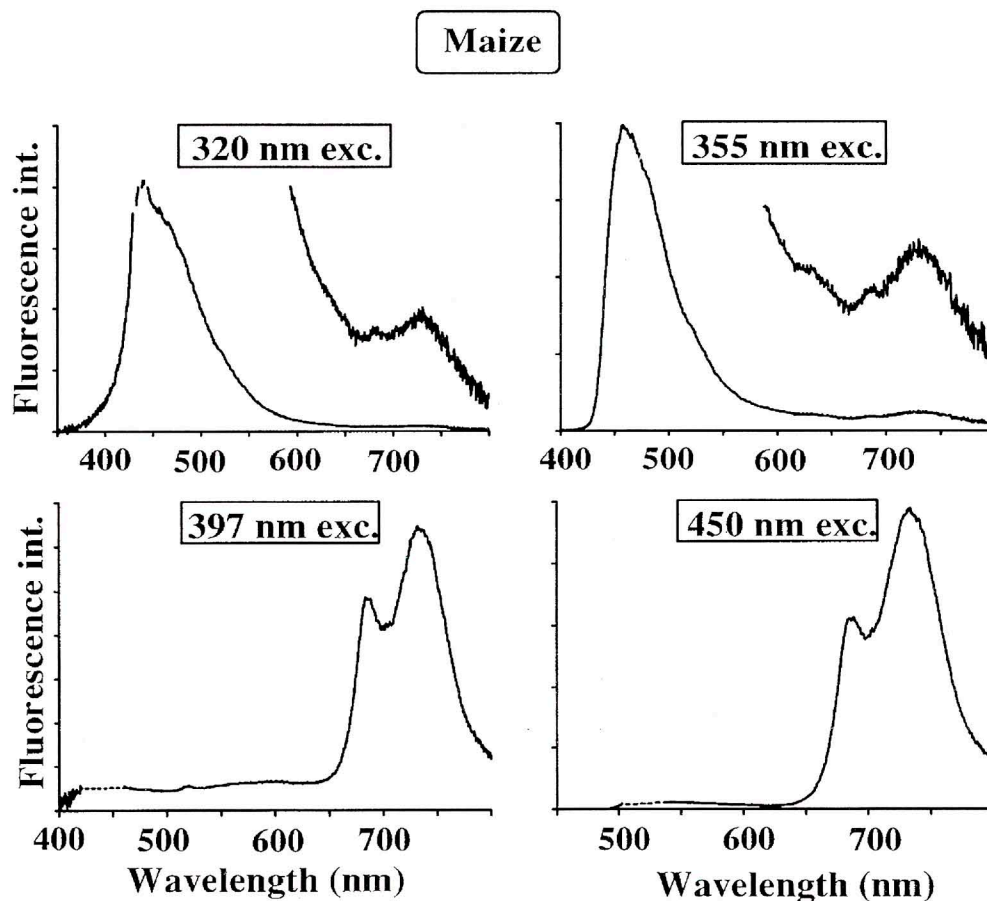


Fig. 3 - Fluorescence spectra from the upper side of a maize leaf recorded inside the van using different excitation wavelengths. A magnification of parts of the spectra of the 320 nm and 355 nm excited spectra are included in the figure.

remote measurements than for the lab measurements. This can be explained by the large target area in the case of remote measurements, for which fluorescence is sampled also from the bark of the branches. In comparison, the lab spectra are taken from isolated leaves and needles only. Another explanation might be that the lab measurements were performed on cut samples, which would enhance the chlorophyll signal. The important observation, though, is that 397 nm excitation yields strong fluorescence in both the red and the blue spectral region.

Remote fluorescence images were recorded for spruce, maize and maple trees. Before attaching the split mirror Cassegrainian telescope, some fluorescence images were recorded at single spectral pass bands, utilizing the full spatial resolution of the CCD detector. The fluorescence images at 685 and 740 nm as well as in the broad blue spectral region are shown for a branch of spruce in Fig. 6. This mode of operation provides a good spatial resolution. However, we were not able to produce a reasonable processed image from division of two of the fluorescence images probably due to slight movements between the recordings.

An example of multi-colour fluorescence imaging of a maize plant is shown in Fig. 7. The image was recorded with interference filters at 685 and 740 nm as well as coloured-glass filters transmitting the broad-band blue and red regions, respectively. Additionally, a processed image, utilizing the images at 685 nm and in the broad-band blue region, is shown below. This technique allows the simultaneous recording of fluorescence images at several wavelengths. Therefore, the processed image is not affected by movement of the detection unit or by spatial intensity fluctuations of the laser, which is a severe problem when recording fluorescence images at different wavelengths in sequence as was done in Fig. 6, or utilizing, for example, a rotating filter wheel. Thus, this technique provides valuable information on vegetation by its image representation of processed fluorescence parameters such as the ratio of the two chlorophyll fluorescence peaks.

The spectral and imaging capabilities were used to extract information about the condition of the plants. Four groups of potted maize plants were investigated; maize grown on sand, maize grown on peat and maize grown with and without nutrient supply. The plants were later analysed and

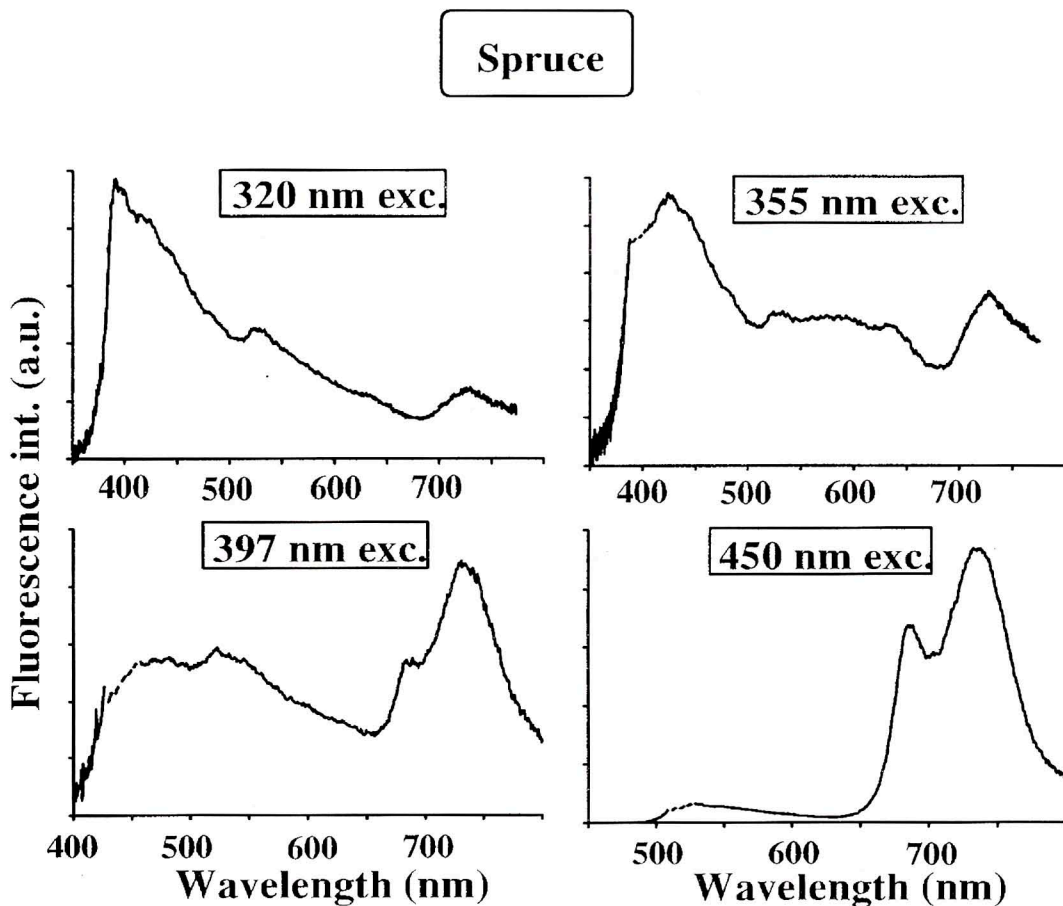


Fig. 4 - Fluorescence spectra from a one year old needle of a spruce recorded inside the van using different excitation wavelengths. A magnification of parts of the spectra of the 320 nm and 355 nm excited spectra are included in the figure.

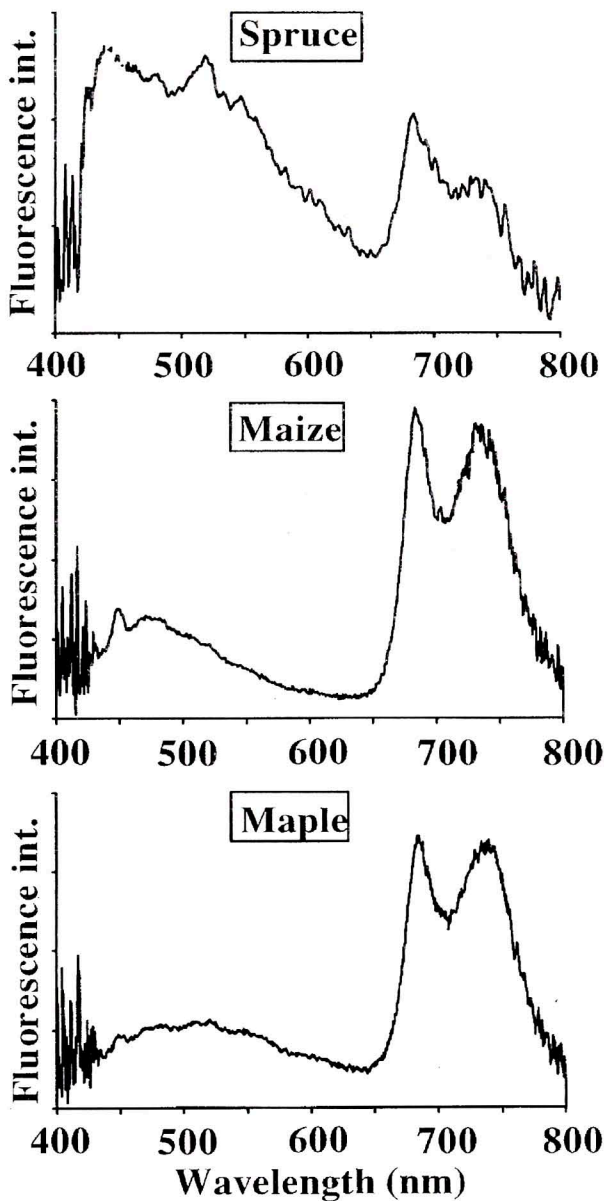


Fig. 5 - Examples of remotely recorded fluorescence spectra for spruce, maize and maple. The excitation wavelength was 397 nm, the target distance about 30 m and the beam diameter about 0.15 m.

the pigment concentration was determined using a chemical extraction procedure. Fluorescence spectra as well as fluorescence images were recorded and the ratio $I(685\text{nm})/I(740\text{nm})$ was evaluated for both methods. As is shown in Fig 8, a gross correlation was found between fluorescence ratio and chlorophyll concentration. The slight disagreement between the two measurement modes is probably due to the fact that in the spectral mode the fluorescence ratio is calculated as an average over a larger area, while the values for the imaging system is calculated for individual leaves.

The daily cycle was followed for spruce and maize, as

shown in Figs. 9 and 10. In the case of spruce, the OMA system was utilized to record fluorescence spectra from 9 a.m. to 11 p.m. In Fig. 9, the filled squares represent the $I(685)/I(740)$ ratio and the open squares the $I(685)/I(480)$ ratio. A slight decrease in the $I(685)/I(740)$ ratio is observed in the afternoon, while for the $I(685)/I(480)$ ratio the level is more or less constant. In the lower part of the figure the global radiation is shown for comparison. In addition, the daily cycle was investigated for maize utilizing the imaging system (Fig. 10). In this case only the $I(685)/I(740)$ ratio was calculated and is shown for two different leaves within the

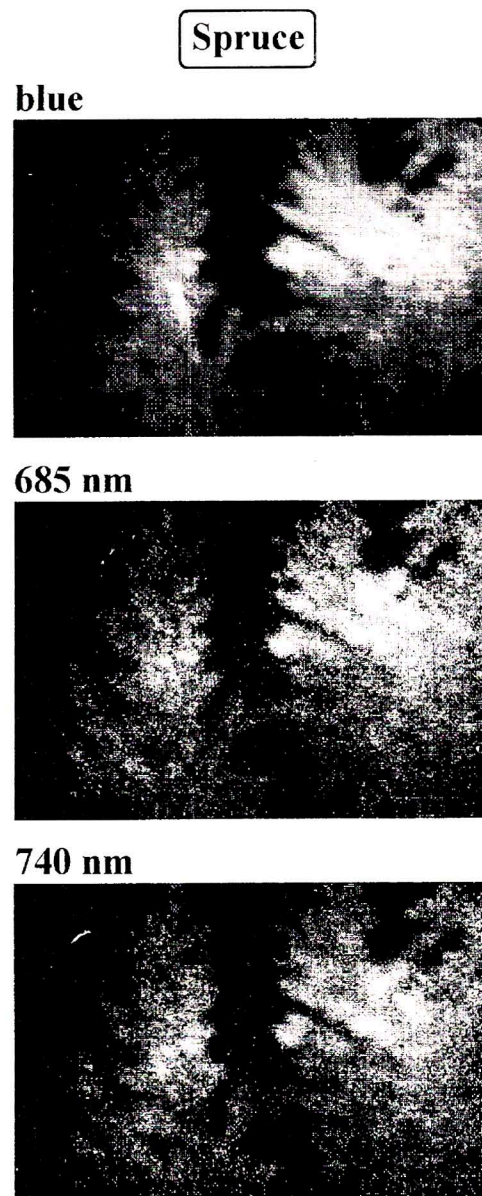


Fig. 6 - Remotely recorded fluorescence images of a branch of a spruce tree. The images were recorded in sequence without the Cassegrainian split-mirror telescope, placing different optical filters in front of the detector. The imaged area was about 1 m in length. The excitation wavelength was 397 nm.

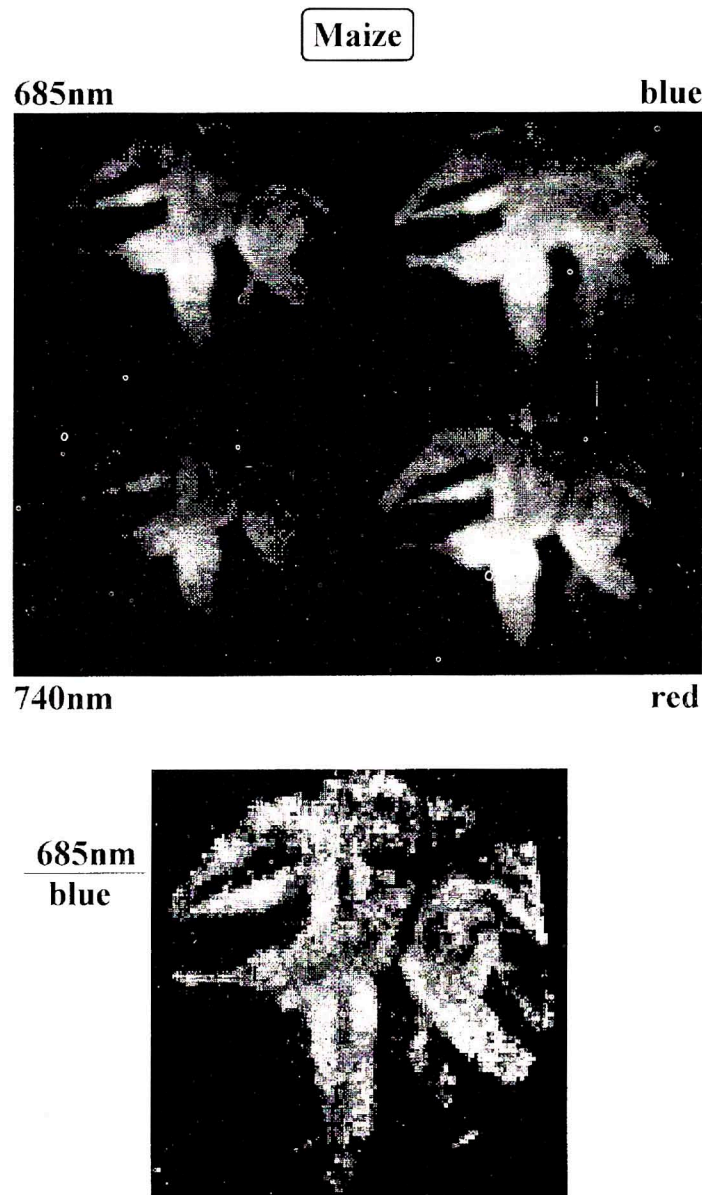


Fig. 7 - Example of multi-colour imaging for a maize plant. The optical filters used in front of each telescope segment were RG665 (red), BG7 (blue), and interference filters centred at 685 and 740 nm, respectively. Below four sub-images, a processed image is shown, displaying the ratio of $I(685\text{nm})/\text{blue}$. The excitation wavelength was 397 nm and the distance was about 30 m. The target diameter was about 0.40 m.

scene. A small increase of the ratio was observed for the maize plants in contrast to the case for the spruce trees.

Some examples of measurements performed at the field campaign in Oberpfaffenhofen have been given above. Beside these examples, more data was collected showing similar results. Maple trees were studied both regarding excitation behaviour and daily cycle. Fluorescence images were recorded for longer distances up to 110 m for spruce trees. In a later set-up of the system the OMA diode array detector was replaced by an image intensified CCD detector and the fibre optic coupling between the telescope and

the spectrometer was changed to a fibre array. With this new arrangement single shot fluorescence spectra could easily be captured at a distance more than 50 m. In conclusion, our measurements showed that spectral as well as spatial information could be obtained from several plant species. Using 397 nm excitation, an effective excitation of chlorophyll as well as blue fluorescence is achieved while still staying eye safe for remote recordings. With the multi-colour imaging technique, it was possible to map a larger area and to display a fluorescence ratio within that area. This technique may be useful for future fluorescence mapping of plant stress.

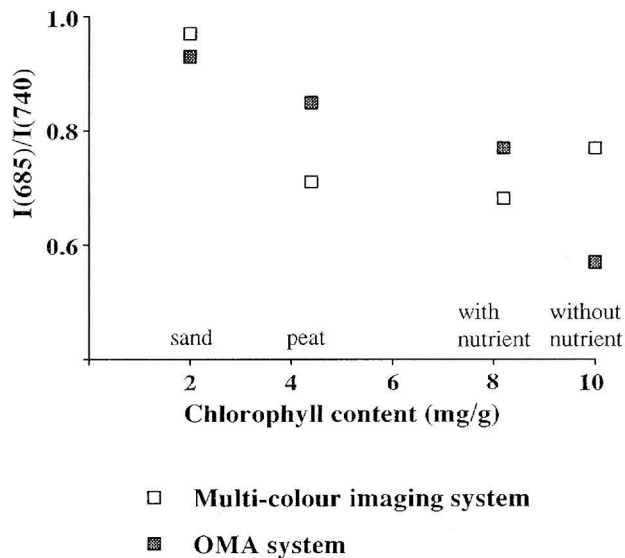


Fig. 8 - Ratio of fluorescence intensities $I(685\text{nm})/I(740\text{nm})$ as a function of chlorophyll content (chl. a + chl. b) within the leaves. The filled squares show the ratio as measured with the OMA system while the open squares represent recordings with the multi-colour imaging system.

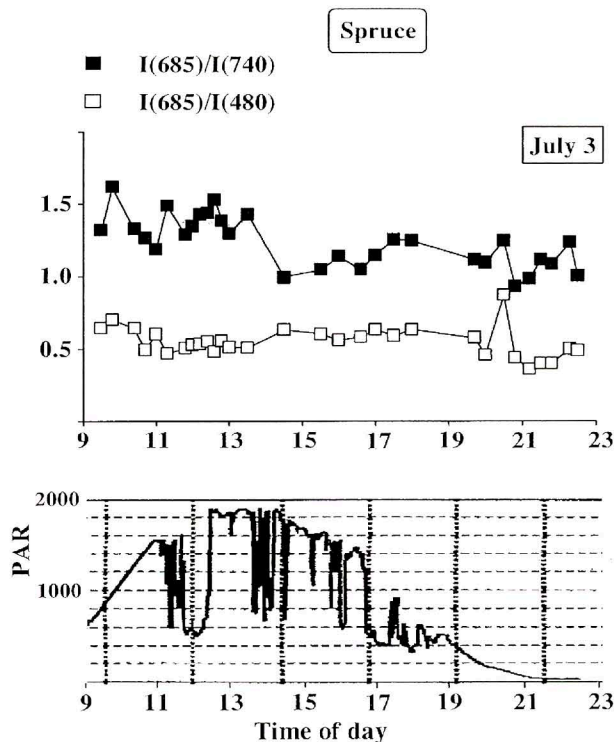


Fig. 9 - Daily cycle variations of the fluorescence ratios $I(685\text{nm})/I(740\text{nm})$ (filled squares) and $I(685\text{nm})/I(480\text{nm})$ (open squares) of spruce trees. Below, the global radiation values are shown for comparison.

ACKNOWLEDGEMENTS

This work was supported by the Swedish Natural Science Research Council and the Swedish Space Board.

REFERENCES

1. B. N. Rock, J. E. Vogelmann, D. L. Williams, A. F. Vogelmann and T. Hoshizaki, "Remote detection of forest damage," *Bio-Science* **36**, 439-445 (1986).
2. L. Pantani and R. Reuter, eds., *Lidar in remote sensing of land and sea*, EARSeL Advances in Remote Sensing **1**, (1992).
3. F. E. Hoge and R. N. Swift, "Airborne simultaneous spectroscopic detection of laser-induced water Raman backscatter and fluorescence from chlorophyll a and other naturally occurring pigments," *Appl. Opt.* **20**, 3197-3205 (1981).
4. F. E. Hoge, R. N. Swift and J. K. Yungel, "Feasibility of airborne detection of laser-induced fluorescence emission from green terrestrial plants," *Appl. Opt.* **22**, 2991-3000 (1983).
5. R. Zimmermann and K. P. Günther, "Laser-induced chlorophyll-a fluorescence of terrestrial plants," in *International Geoscience and Remote Sensing Symposium IGARSS'86*, (ESA Publications Division, Noordwijk, 1986), 1609-1613.
6. L. Celander, K. Fredriksson, B. Galle and S. Svanberg, "Investigation of laser-induced fluorescence with applications to remote

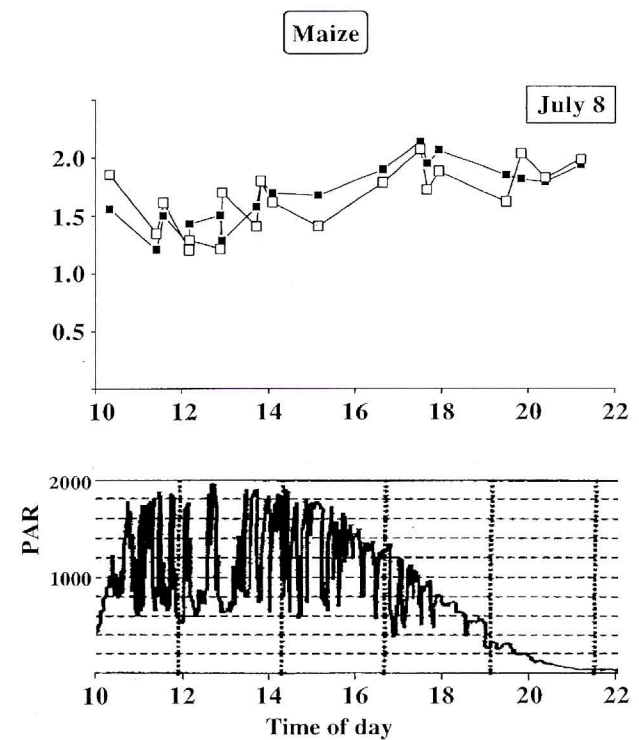


Fig. 10 - Daily cycle variations of the fluorescence ratio $I(685\text{nm})/I(740\text{nm})$ for two different leaves of a maize plant measured by the multi-colour imaging system. Below, the global radiation values are shown for comparison.

- sensing of environmental parameters," Göteborg Institute of Physics Reports, GIPR-149, Göteborg (1978). See also: S. Svanberg, "Laser fluorescence spectroscopy in environmental science, in *Optoelectronics for Environmental Science*, S. Martellucci and A.N. Chester, eds., 15-27, Plenum Press, N.Y. (1989).
7. A. Rosema, G. Cecchi, L. Pantani, B. Radicati, M. Romuli, P. Mazzinghi, O. van Kooten, C. Kliffen, "Results of the 'LIFT' project: Air pollution effects on the fluorescence of Douglas fir and poplar," in *Applications of chlorophyll fluorescence*, H.K. Lichtenthaler, ed., 307-317, Kluwer Academic Publishers, Dordrecht, (1988).
8. H. Edner, J. Johansson, S. Svanberg, E. Wallinder, M. Bazzani, B. Breschi, G. Cecchi, L. Pantani, B. Radicati, V. Raimondi, D. Tirelli, G. Valmori, P. Mazzinghi, "Laser-induced fluorescence monitoring of vegetation in Tuscany," *EARSel Advances in Remote Sensing*, **1**, 119-130 (1992).
9. H. K. Lichtenthaler and U. Rinderle, "The role of chlorophyll fluorescence in the detection of stress conditions in plants," *CRC Critical Reviews in Analytical Chemistry* **19**, S29-S85 (1988).
10. E.W. Chappelle, J.E. McMurtrey and M.S. Kim, "Laser induced blue fluorescence in vegetation," in *Proc. Internat. Geoscience Remote Sensing Symposium IGARSS '90* **3**, 1919-1922, University of Maryland, Washington DC (1990).
11. M. Lang and H.K. Lichtenthaler, "Changes in the blue-green fluorescence-emission spectra of beech leaves during the autumnal chlorophyll breakdown," *J. Plant Physiol.* **138**, 550-553 (1991).
12. L. N. M. Duysens and G. Sweep, "Fluorescence spectrophotometry of pyridine nucleotide in photosynthesizing cells," *Biochim. Biophys. Acta* **25**, 13-16 (1957).
13. Y. Goulas, I. Moya and G. Schmuck, "Time-resolved spectroscopy of the blue fluorescence of spinach leaves," *Photosynth. Res.* **25**, 299-307 (1990).
14. H. Schneckenburger and M. Frenz, "Time-resolved fluorescence of conifers exposed to environmental pollutants," *Radiat. Environ. Biophys.* **25**, 289-295 (1986).
15. H. Edner, J. Johansson, S. Svanberg and E. Wallinder, "Fluorescence lidar multi-color imaging of vegetation," *Appl. Opt.* **3**, 2471-2479 (1994).